Supplementary Information

Precise tuning of bacterial translation initiation by non-equilibrium 5'-UTR unfolding observed in single mRNAs

Sujay Ray†, Shiba S. Dandpat, Surajit Chatterjee and Nils G. Walter*

Single-Molecule Analysis Group, Department of Chemistry, University of Michigan, Ann Arbor, MI 48109, USA. *e-mail: nwalter@umich.edu, † Current address: Wyss Institute for Biologically Inspired Engineering at Harvard University.

Materials and Methods

Ribosome Preparation. Mutant *E. coli* pKK3535 plasmid strain with an extension at the helix-44 of the 16s rRNA was obtained from Joseph Puglisi's laboratory. This extension allows labeling of the ribosome using a fluorescently labeled DNA oligonucleotide complementary to the extended portion of the helix-44 without affecting the ribosome's functionality[1]. The helix extension presence was further verified by sequencing the plasmid. To confirm that the strain contains only mutated ribosome where the 16S ribosomal RNA contains the extension, total RNA was extracted from a small culture of cells following previously published protocol. The extracted RNA was then verified by reverse transcription followed by DNA-sanger sequencing. Single salt-washed ribosomes were prepared using a previously described protocol with several modifications[1]. Briefly, the pKK3535 strain, containing mutated ribosome was grown in Luria-Bertani (LB) medium at 37 °C to an OD_{600} of 0.8-1 starting from an overnight culture. The cells were then cooled at 4 °C for 45 min and pelleted at 5,000 rpm for 15 min. All subsequent steps were performed on ice or at 4 °C. The cell pellet was resuspended in buffer A (20mM Tris-HCl (pH 7.05 at 25 °C), 100 mM NH_4Cl, 10 mM $MgCl_2$, 0.5 mM EDTA and 6 mM β-mercaptoethanol), and the cells were lysed in a single pass using a M-110L Microfluidizer processor (Microfluidics). The lysate was cleared by centrifugation at 16,000 rpm in a JA-20 rotor. The clarified lysate was pelleted over a 35-ml sucrose cushion (1.1 M sucrose, 20 mM Tris-HCl (pH 7.05 at 25 °C), 500 mM NH_4Cl, 10 mM $MgCl_2$ and 0.5 mM EDTA) in a Beckman Ti-45 rotor for 16-20 hours overnight at 37,000 rpm. The pellet was washed twice with 1ml of buffer B (20 mM Tris-HCl (pH 7.05 at 25 °C), 500 mM NH_4Cl, 10 mM $MgCl_2$ and 0.5 mM EDTA), resuspended in 6 ml of buffer B by gentle stirring. The one salt-washed 70S ribosomes were then dialyzed against low magnesium buffer E (50 mM Tris-HCl (pH 7.05 at 25 °C), 150 mM NH_4Cl, 1 mM $MgCl_2$ and 6 mM β-mercaptoethanol) three times. The low Mg^{2+} ions facilitate the two subunits to dissociate from each other and remain as individual subunits in the solution. Next, 100 A_{260} unit of the dissociated ribosome is loaded onto a 36 ml of previously prepared sucrose gradient (to prepare the gradient, buffer E + 20% sucrose is frozen at -80 °C and then gently thawed at room temperature without mixing). The gradients were then loaded onto a swinging bucket (SW-28) rotor and centrifuged at 20,000 rpm for 18 hours. The gradients were then fractionated using a Brandel gradient fractionator coupled with a UV-detection monitor. Appropriate fractions were

pooled together as pure 30S and pure 50S fractions. The 30S and 50S fractions were then pelleted separately for 12 hours at 66,000 rpm in a Beckman Ti-70 rotor. Pelleted subunits were resuspended in storage buffer (50 mM Tris-HCl (pH 7.5 at 25 °C), 70 mM NH_4Cl, 30 mM KCl, 7 mM $MgCl_2$ and 6 mM β-mercaptoethanol) and flash-frozen with liquid nitrogen and stored at -80 °C.

Labeling of 30S ribosomal subunit. To observe direct binding of the 30S to the nascent mRNA, we doubly labeled the *E. coli* 30S with Cy5 by hybridizing a dual Cy5 labeled DNA oligonucleotide (Supporting table S1) to an engineered extension in the helix 44 of the 16S rRNA[1]. The 30S labeling was performed with a 10-fold excess of dual-Cy5 labeled DNA oligonucleotide (IDT), at a final 30S concentration of 1 μM and a buffer composition (50 mM Tris-OAc (pH 7.5 at 25°C), 100 mM KCl, 5 mM NH_4OAc, 0.5 mM $Ca(OAc)_2$, 5 mM $Mg(OAc)_2$, 6 mM β-mercaptoethanol, 0.5 mM EDTA, 5 mM putrescine, and 1 mM spermidine) which has been optimized for activity of purified ribosomes[2]. The reaction was protected from light and incubated for 10 min at 37°C, then 60 min at 30°C and finally cooled gradually to room temperature. Excess fluorescent oligonucleotides were then removed by spin column (Millipore, UFC510024) and the solution containing the labeled 30S was flash-frozen in aliquots and stored at -80°C. The final concentration of the 30S in the recovered solution was determined spectrophotometrically using the extinction coefficient ε_{260} = 14492753.62 $M^{-1}cm^{-1}$ for 30S and ε_{650} = 250000 $M^{-1}cm^{-1}$ for Cy5.

Initiation complex formation assay. 30S initiation complexes were prepared by mixing 1 μM R-mRNA^{FL} or truncations (R-mRNA^{+30} and R-mRNA^{-11}), 2 mM GTP, 3 μM each of IF1, IF2 and IF3, 3 μM ^{32}P-fMet-tRNA^{fMet}, 1 mM $MgCl_2$, 1.5 μM twice salt-washed 30S ribosomes, and Tris-polymix buffer, composed of 50 mM Tris-OAc (pH 7.5 at 25 °C), 100 mM KCl, 5 mM NH_4OAc, 0.5 mM $Ca(OAc)_2$, 5 mM $Mg(OAc)_2$, 6 mM β-mercaptoethanol, 0.5 mM EDTA, 5 mM putrescine, and 1 mM spermidine (the total Mg^{2+} concentration in the reaction from all of the added components was ~7.5 mM). Reactions were incubated in a 37°C water bath for 50 min and then the radioactive counts in 1 μL of the reaction were measured by scintillation counting. Successfully formed 30S ICs were purified away from unincorporated initiator tRNA and initiation factors by carefully layering the sample onto a 1.3 mL sucrose cushion (1.1 M sucrose, Tris-polymix buffer, 15 mM $MgCl_2$, 0.5 mM EDTA) in an ultracentrifuge tube, and centrifuged in a Beckman TLA-100.3 rotor at 69,000 rpm for 2.5 h at 4°C. The supernatant was carefully removed,

and the pelleted material was resuspended by gentle pipetting in 40 µL of Tris-polymix buffer. The radioactive counts in 1 µL of the resuspended material were measured by scintillation counting and the efficiency of 30S IC formation was calculated by taking the ratio of counts after and before centrifugation.

Cloning of sequences encoding the R-mRNA and different mutants. The complete mRNA transcript, including the TTE_RS07450 and TTE_RS07445 (TTE1564 and TTE1563, respectively) ORFs, and its 30 UTR as predicted from the FindTerm algorithm (Soft-Berry), was amplified using PCR from *T. tengcongensis* genomic DNA, which was purchased from the NITE Biological Resource Center. The amplified region was cloned into the pUC19 plasmid between the BamHI and HindIII sites with an engineered upstream T7 promoter (pUC19_*Tte*). Different lengths of DNA were prepared by PCR amplification of the desired parts of the DNA. DpnI enzyme, which cleaves methylated DNA, is used to digest parent plasmid. 2′-O-methylation (2′-OMe) modification in the first two bases of the reverse primers ensures that during transcription in the next step, RNA polymerase dissociate without adding additional bases at the 3' end of the RNA. Transcription reactions were performed in the presence of 120mM HEPES-KOH (pH 7.5 at 25°C), 30 mM $MgCl_2$, 2mM spermidine, 40mM dithiothreitol (DTT), 30mM NTPs, 0.01% (w/v) Triton X-100, 400nM PCR amplified DNA, 0.01U/ml pyrophosphatase and 0.2 mg/ml T7 RNA polymerase in a total volume of 150 µl. Transcription reactions were incubated at 37°C for ~ 18 h. mRNA was purified by denaturing, 7M urea, PAGE, detected using brief 254-nm ultraviolet radiation and gel-eluted overnight. mRNAs were ethanol-precipitated and resuspended in water.

Different R-mRNA mutations were generated from the original pUC19_Tte plasmid. PCR based site-directed mutagenesis was performed with primers (Supplementary Table S1 for RNA sequences and Table S5 for primer sequences) designed to span the mutated bases. RNAs were generated from the plasmids in the same way as described above.

3' fluorophore labeling of RNA. RNA constructs prepared by transcription as described above were labeled with a Cy3 fluorophore at their 3' end following a method described previously by Willkomm and Hartmann[3] with several modifications. Briefly, RNA constructs were first oxidized by incubating 5 µM RNA in 100 mM NaOAc (pH 5.2) with freshly prepared 2.5 mM sodium (meta) periodate (Fluka, 71859) on ice for 70 min, protected from light.

Subsequently, the oxidized RNA was precipitated with the addition of 0.1 V of 3 M NaOAc (pH 5.2) and 2.5 V of cold absolute ethanol, followed by incubated on dry ice until frozen. The solution was inverted until just thawed and then centrifuged at 20,800 × g for 45 min at 4 °C to pellet the RNA. The supernatant was removed by pipetting, and the pellets were then washed with ~0.3 V of cold 70% (v/v) ethanol and centrifuged again for 20 min. The wash was removed by pipetting and the pellets were dried under vacuum. The oxidized RNA was then coupled with a hydrazide derivative of the fluorophore Cy3 (GE Healthcare, PA13120). A typical 100 µL coupling reaction contained ~0.2 – 1.0 nmol of RNA, 50 nmol of Cy3 hydrazide (dye) dissolved in 10 µL of DMSO, and 100 mM NaOAc (pH 5.2). Solutions were degassed prior to the addition of dye, and the headspace above fully assembled reactions was flushed with nitrogen before capping the reaction tube. Reactions were protected from light and incubated at room temperature for 4 hr with agitation. In all subsequent steps, solutions were protected from light. After the end of the incubation, the Cy3-labeled RNA was precipitated with the addition of 0.1 V of 3 M NaOAc (pH 5.2) and 2.5 V of cold absolute ethanol, followed by incubated on dry ice until frozen. The solution was inverted until just 88 thawed and then centrifuged at 20,800 × g for 45 min at 4 °C to pellet the RNA. The supernatant was removed by pipetting, and the pellets were then washed with 2 V of cold 70% ethanol and centrifuged again for 20 min. The wash was removed by pipetting and the pellets washed again with 0.5 V of cold 70% ethanol and centrifuged again for 15 min. This final wash was removed by pipetting and the RNA pellets were dried under vacuum and resuspended in 30 µL cold milliQ water, and then desalted using Illustra MicroSpin G-50 columns that had been preequilibrated in milliQ water. The final concentration of RNA in the recovered solution was determined spectrophotometrically using a Nanodrop2000 spectrophotometer, using the respective extinction coefficient at 260 nm (ε_{260}) for the RNA (945,180 M^{-1} cm^{-1}) and ε_{550} = 150,000 M^{-1} cm^{-1} for Cy3. The contribution of dye to the absorbance at 260 nm was accounted for as follows: A260, RNA = A260 - 0.08 × A550.

RNA filter binding assay: The principle for this assay is based on the double-filter method described before, in which the binding of radiolabeled nucleic acids by proteins or other macromolecules is assessed by filter binding reactions through a pair of stacked membranes and measuring the amount of radioactivity retained in each[4-6].

Radiolabeled R-mRNA^{+30} was prepared in two steps. In the first step, 5 µM RNA was dephosphorylated using Antarctic phosphatase enzyme (New England Biolab). The reaction was incubated at 37°C for 30 min, followed by heat deactivation for 2 min at 80°C. In the second step, dephosphorylated RNA was phosphorylated using ^{32}P-labeled ɣ-ATP and T4 Poly Nucleotide Kinase (NEB). The reaction was incubated at 37°C for 30 min. The resulting radiolabeled RNA was purified by a spin column.

Twice salt-washed 30S subunits used for all assays were activated by incubation at 37°C in the Tris-polymix buffer for 5 min immediately prior to use. For each reaction, 3 µL of 3 mM R-mRNA^{+30} was re-folded in the absence and presence of 1 µM preQ$_1$ by heating to 70°C for 2 min, followed by slow cooling to room temperature for 15 min. 30S subunits in Tris-polymix buffer was added to the RNA with and without preQ$_1$ at different time interval into the filtration column.

Membranes were pre-wet in binding buffer for 30 min. A membrane stack was constructed by stacking (from top to bottom): a reinforced nitrocellulose membrane (Optitran BA-S 85, Whatman #10-439-191), a Whatman 1MM filter paper, a positively-charged nylon membrane (BrightStar-Plus, Ambion), and a second Whatman 1MM filter paper. The membrane stack was clamped inside of 96-well dot-blot manifold (Mini-fold, Schleicher & Schuell) and were then washed with cold binding buffer (100 µL per well) and dried by applying vacuum.

The 30S and RNA binding reactions were pipetted into the wells of the manifold, drawn through the membranes under vacuum, and then washed 100 µL cold buffer. Vacuum was applied for 2-3 min until the membranes appeared dry and then membranes were wrapped in saran wrap and imaged using a storage phosphor screen and Typhoon 9410 Variable Mode Imager (GE Healthcare Life Sciences) and quantified using ImageQuant v 5.2 (Molecular Dynamics). Radiolabeled RNA that is successfully incorporated into the 30S-RNA complex is preferentially retained in the nitrocellulose filter, while unbound tRNA is trapped in the positively charged nylon filter. The fraction of bound and unbound 30S were calculated as described previously[5].

Single-molecule fluorescence microscopy. A prism-type total internal reflection fluorescence setup built around an Olympus-IX83 microscope, equipped with 60× 1.20 N.A. water objective and four sCMOS cameras (Hamamatsu,

Flash-4 V3) and four different wavelength laser lines was used to perform the ribosome binding experiments (Only two laser lines and two cameras are used). Flow cell sample channels were prepared on surface passivating quartz microscope slides though coated with a mixture of 90% methoxy Poly-Ethelyn Glycol succinimidyl valeric acid (m-PEG SVA) and 10% biotin-PEG succinimidyl valeric acid (biotin-PEG SVA) using previously established protocols[7,8]. For surface immobilization of R-mRNA, the sample chamber was treated with 0.2 mg/mL streptavidin to bind to the biotin from the PEG. Solution containing ~50 pM previously annealed biotinylated capture strand-RNA complex was introduced to the chamber to sparsely coat the PEG surface with streptavidin. Excess non-immobilized RNAs were then washed with 200 µL wash buffer (10 mM Tris Base, pH 7.5 @ 25 °C). Steady-state SiM-KARB and ribosome binding measurements were performed by first forming the riboswitches by incubating the surface-immobilized RNA constructs with at a given concentration of $preQ_1$ in Tris-polymix buffer for 15 min. 20 nM concentration of dual Cy-5 labeled ribosome solution with same concentration of $preQ_1$ was then added to the chamber in an imaging solution (Tris-polymix buffer, 5 mM protocatechuic acid and 50 nM protocatechuate-3,4-dioxygenase, 2 mM Trolox). The dual labeling ensured long binding events of 30S to R-mRNA despite photobleaching of individual Cy5 molecule. An integration time of 100 ms was used unless otherwise specified for the experiments. A combination of continuous and shuttered illumination was used to capture slow and fast dynamic events, respectively. Shuttered illumination was specifically used for non-equilibrium ligand-jump experiments. Ten thousand frame movies at the rate of 100 ms per frame (150 ms per frame for mutants due to long observed binding times of 30S to mutants) were recorded for each condition with continuous 532 nm and 639 nm laser sources for the whole duration.

Ligand-Jump Experiment. Surface immobilized R-mRNA^{+30} molecules in the absence of $preQ_1$ were first introduced to buffer containing 20 mM of Cy5 labeled 30S and monitored for eight hundred seconds, followed by six hundred seconds dark time (shown in gray, Fig. 3A). During the dark period, a fresh buffer solution containing 1 µM $preQ_1$ and same concentration of Cy5-30S as before was injected. The dark period allowed time for the homogeneous exchange of buffer and OSS to reduce photobleaching probability. After the dark period, molecules in the same

field of view were tracked in real-time for another eight hundred seconds in the presence of the $preQ_1$ without altering the preexisting concentration of buffer and 30S in the solution.

Analysis of Single-molecule Data. Single-molecule time traces were generated by a custom-written MATLAB code. Furthermore, custom analysis programs in MATLAB were used to extract statistical data from individual molecules, and finally Origin Pro9 was used to plot the data.

Global fitting. All the data for association and dissociation rates for each condition were fitted together globally in Origin pro software to get higher accuracy of double-exponential fitting[9,10]. To reduce the number of independent parameters associated with double-exponential fitting for both association and dissociation rates as well as considering the heterogeneity of the 30S binding to the R-mRNA^{+30} for each condition, the shorter binding time of the double-exponential fitting was shared across all the conditions of $preQ_1$ and effect of mutations. The global fitting of rates separately yielded two components for each of association ($k_{on,\ slow}$ and $k^{shared}{}_{on,\ fast}$) and dissociation ($k_{off,\ slow}$ and $k^{shared}{}_{off,\ fast}$) rates, one of which was variable, and the other was shared over all the conditions. While the shared component of the rate constant (k^{shared}) remained fixed for all conditions, the variable component was observed to be profoundly responsive to the influence of $preQ_1$. The variable rate constant components and their relative contributions were used to compare different conditions to determine the role of $preQ_1$ and strategic mutations on 30S ribosome binding.

Distributions of High (H), Mid (M), Low (L) groups of molecules. For 30S binding to R-mRNA^{+30}, three types of 30S binding time distribution were observed by plotting an accumulated distribution of total binding time of 30S for all the conditions pooled together (Supplementary Fig. 4). The cumulative binding time histograms were fitted with three Gaussian plots (with R-Sq value of 0.9914), showing there are three types of total binding populations, which were assigned as H, M, and L to represent the binding regime they cover. The population H represented the high-range of binding time of the 30S (>30% of the total observation window), M represented mid-range binding time (between 20-30% of the total observation window) and L represented low-range binding time (<10% of the observational window). These regions for H, M, and L were used as cutoffs for calculating cumulative or

percentage population for each condition. The cumulative or percentage population for each regime was calculated for each condition by counting the total binning for each regime.

Rastergram distributions. For determining the nature and number of standby (short) and cleft-accommodated (long) binding events, we represented a random selection of 100 molecules for each condition in a rastergram[11,12]. First, the molecules were clustered into H, M, and L groups by analyzing the total binding time of the 30S each molecule categorized from the cutoffs estimated from the total binding time histogram distributions shown for each condition. To categorize the binding events into standby (red) and cleft-accommodated (blue) binding events, we took the geometric mean of the two components of binding times obtained from the double-exponential fitting of the cumulative plot for the binding times obtained earlier. We then counted the number of red and blue events for the required conditions and used them to compare any change in the nature of 'standby' and 'cleft-accommodated' binding events under the influence of $preQ_1$ or the effect of strategic mutations. We plotted each individual molecule's 30S binding behavior categorized into the groups of H, M, and L to represent binding events as standby or cleft-accommodated events (shown in red or blue) within each condition. MATLAB scripts for raster plots are available upon request.

S1 depletion and labeling of 30S Ribosome. 30S subunits depleted of S1 (ΔS1-30S) were prepared following a method adapted from Lauber *et al.* Briefly, because S1 has a high affinity for polyU RNA, it can be efficiently removed from the 30S subunit by incubation with polyU resin. 125 mg of polyuridylic acid–agarose resin (Sigma, P8563) was swelled in 15 mL of polyU wash buffer (20 mM Tris-HCl, pH 7.5 at 25°C, 100 mM NaCl) in a Poly-Prep chromatography column (Bio-Rad, 7311550). All subsequent steps were performed at 4°C or ice to prevent degradation of the polyuridylic acid. The column was placed inside of a 15 mL Falcon tube and centrifuged in a swinging bucket rotor at 100 × g for 1 min. The column was then washed by adding 1 mL of polyU wash buffer and centrifuging for an additional minute. This wash step was repeated 12 times in total to extensively remove loosely bound or degraded polyU RNA from the column. The column was then equilibrated with six 1mL washes with S1-depletion buffer (20 mM Tris-HCl, pH 7.5 at 25°C, 1M NH_4Cl, 10 mM $MgCl_2$, 60 mM KCl, and 1 mM DTT).

Supplementary Figures

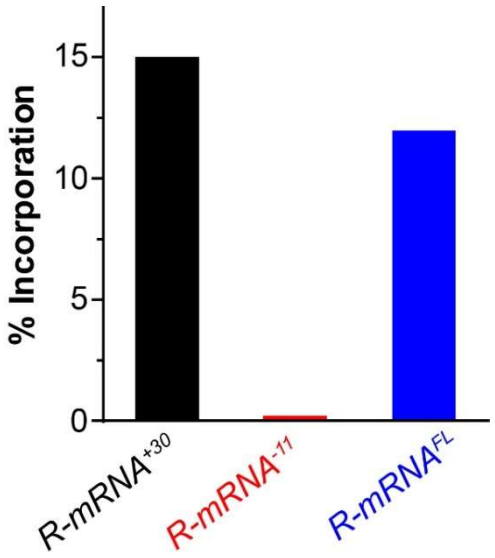

Supplementary Fig. 1| R-mRNA truncations to determine RNA required for 30S IC formation. Comparison of 30S IC formation efficiency on full length R-mRNA^{FL} and R-mRNA^{+30} truncation and R-mRNA^{-11} truncation (no SD/ ORF). As expected, ICs do not form on mRNA that lacks a SD and ORF, whereas efficiency of initiation is similar for full length R-mRNA and R-mRNA^{+30}.

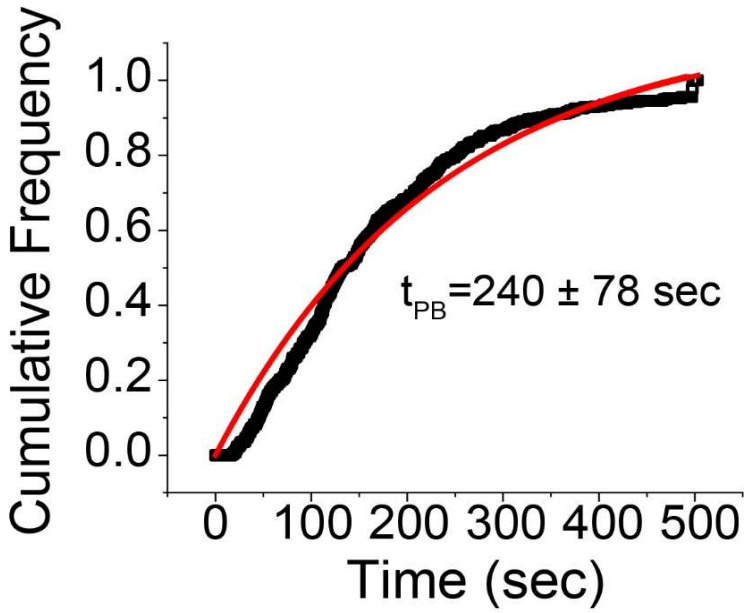

Supplementary Fig. 2| Characterization of photobleaching time for 30S labeling probe. The dual Cy5 labeled 30S labeling-oligo was captured on the surface by a biotinylated capture strand. Same assay conditions and laser intensity and optical parameters were maintained as the SiM-KARB assays. The average characteristic photobleaching time is shown in the graph, which is an estimation of photobleaching of both dye molecules.

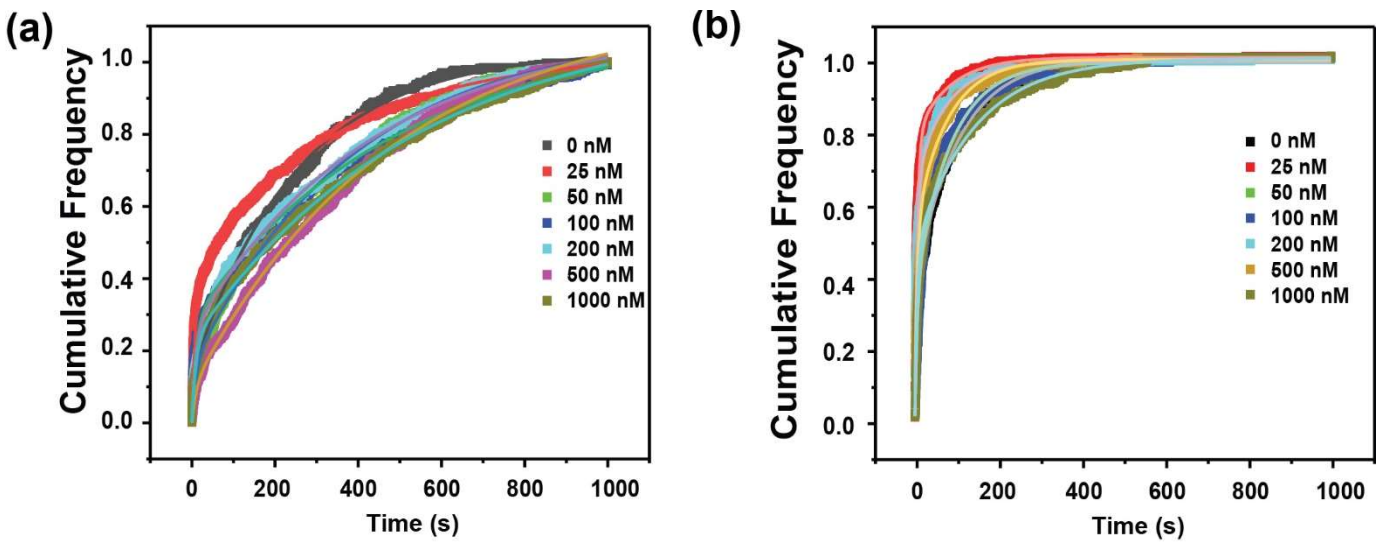

Supplementary Fig. 3| Plots of cumulative unbound (A) and bound (B) dwell times for the 30S binding at different concentrations of preQ$_1$

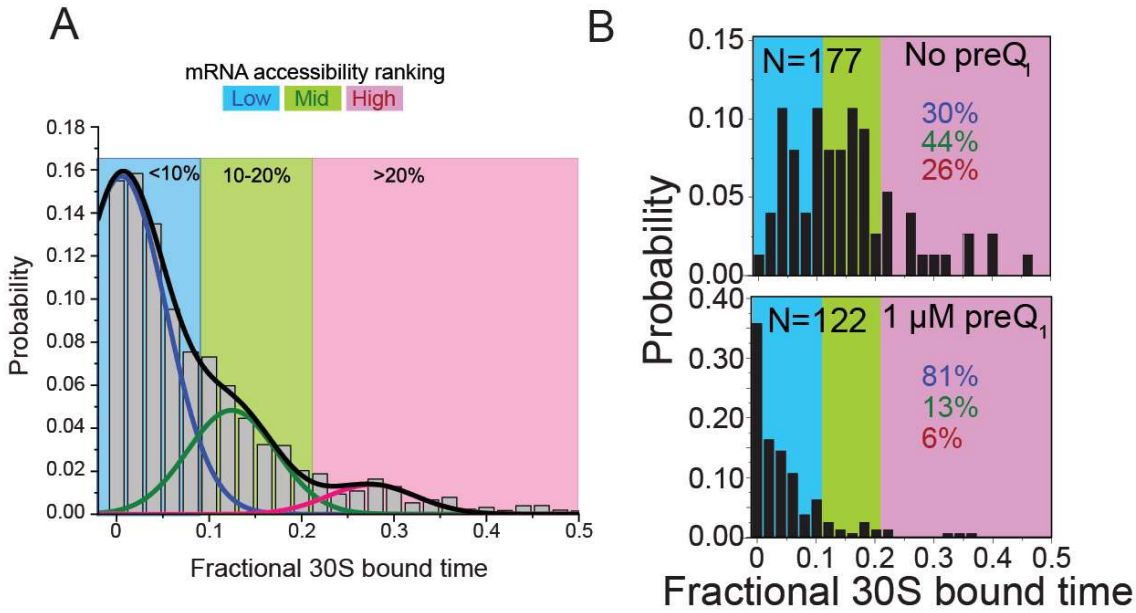

Supplementary Fig. 4| (A) Cumulative plot of all histograms pooled together to identify distribution of bound time populations. (B) Example of histogram plot for mRNA accessibility.

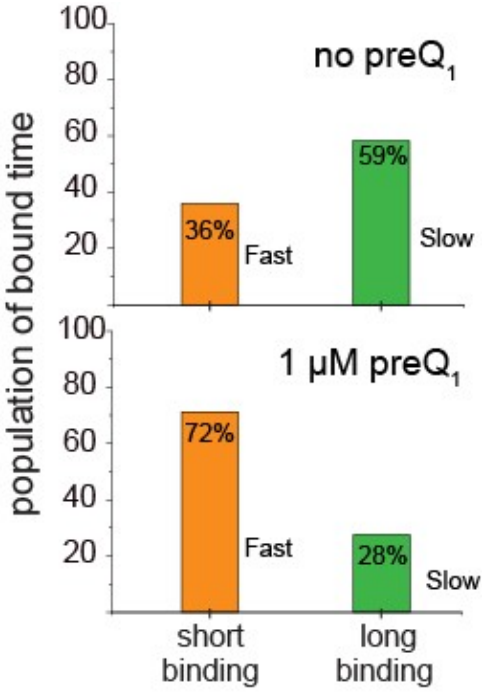

Supplementary Fig. *5*|Percentage of long and short binding events for 30S binding to R-mRNA^{+30} in the absence and presence of preQ$_1$ determined from the biexponential fitting of the association ($k_{on,\ slow}$) and dissociation ($k_{off,\ slow}$) rates

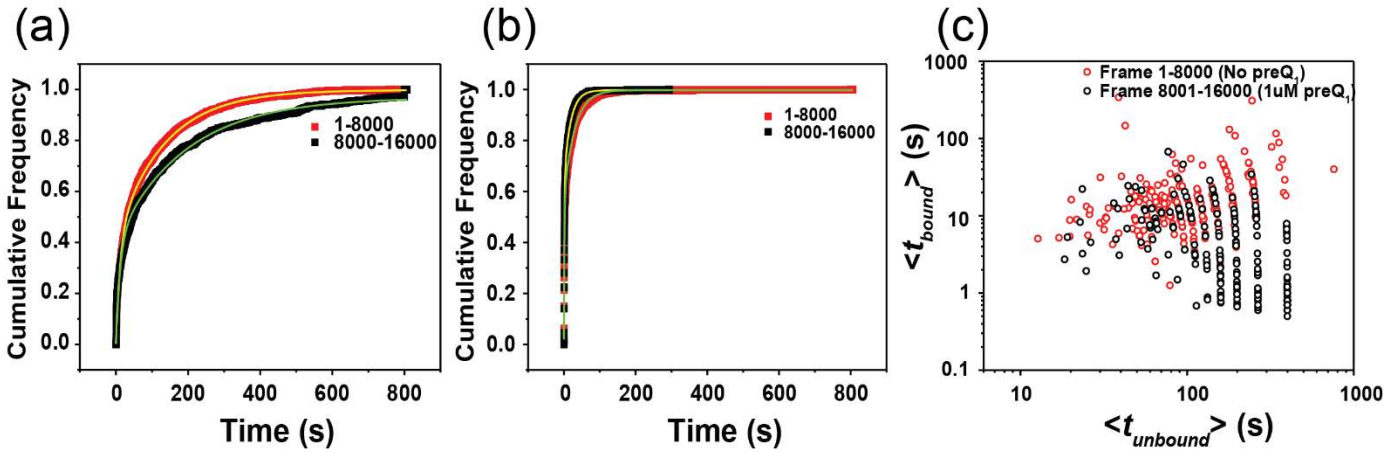

Supplementary Fig. 6| Plots of cumulative unbound and bound dwell times for the 30S binding without and with preQ$_1$ in ligand-jump experiments. (a) Cumulative frequency plot for $t_{unbound}$ of 30S binding to R-mRNA^{+30} without preQ$_1$ (red) before dark period monitored for first 8000 frames and with 1 μM preQ$_1$ (black) after dark period monitored for next 8000 frames. 1 μM preQ$_1$ is added during the dark period that lasts for 5000 frames (1 frame = 0.1 sec) (b) Cumulative frequency plot for t_{bound} of 30S binding to R-mRNA^{+30} without PreQ$_1$ (red) and with 1 μM preQ$_1$ (black) (c) Scatter plot between average unbound time ($t_{unbound}$) vs average bound time (t_{bound}) obtained from the non-equilibrium ligand-jump experiment showing an increase in avg. $t_{unbound}$ and t_{bound}.

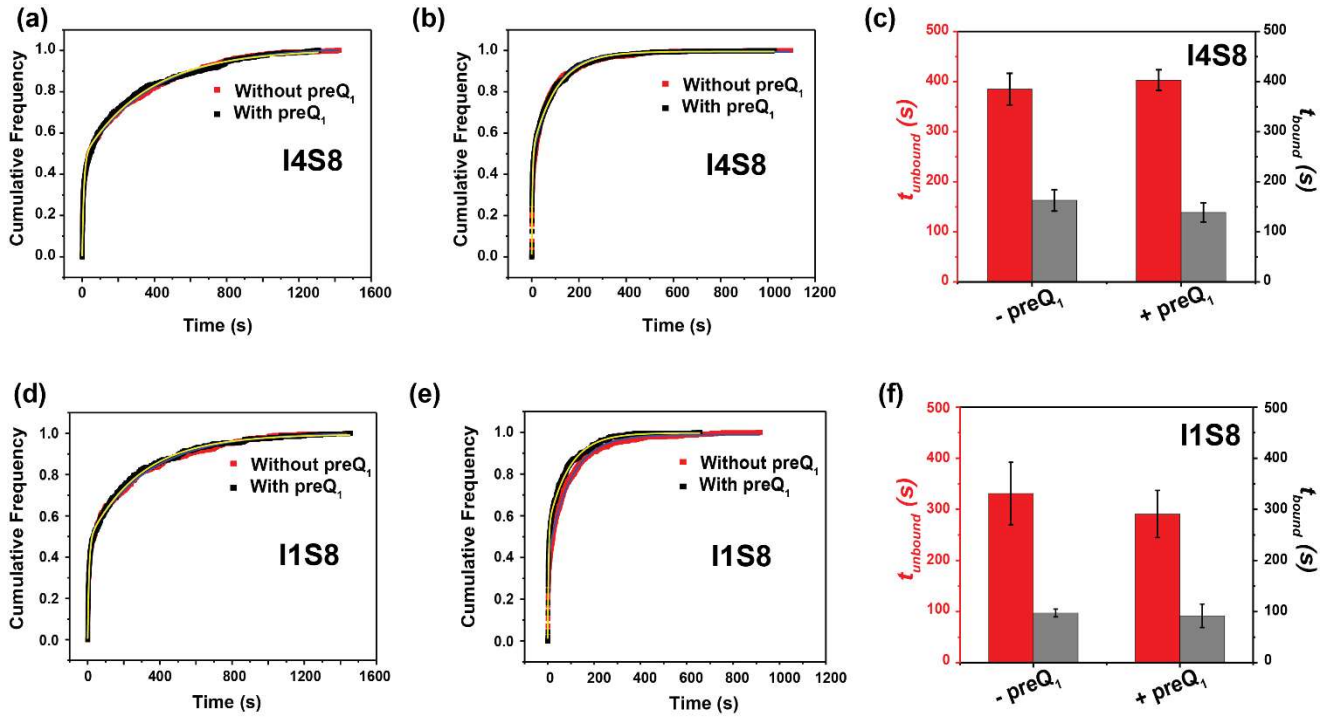

Supplementary Fig. 7| *Effect of preQ$_1$ on mutants I4S8 and I1S8.* (a) Cumulative frequency plot for $t_{unbound}$ for I4S8 in absence and presence of preQ1; (b) Cumulative frequency plot for t_{bound} for I4S8 in the absence and presence of preQ$_1$. (c) Comparison of OFF and ON time for I4S8 without and with preQ$_1$. (d) Cumulative frequency plot for $t_{unbound}$ for I1S8 in the absence and presence of preQ$_1$; (e) Cumulative frequency plot for t_{bound} for I1S8 in the absence and presence of preQ$_1$; (f) Comparison of unbound ($t_{unbound}$, red) and bound (t_{bound}, red) time for I1S8 in the absence and presence of preQ$_1$.

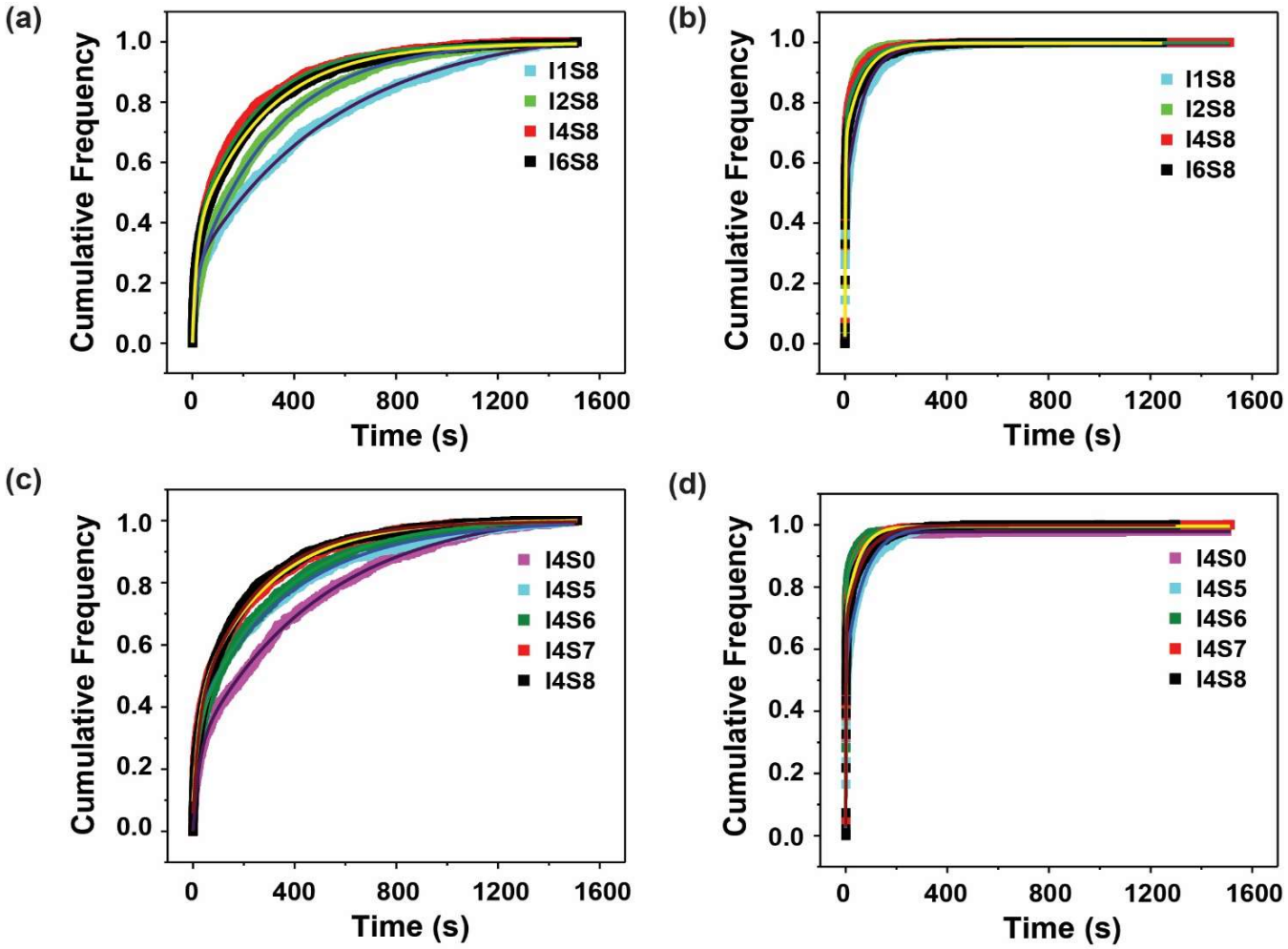

Supplementary Fig. 8| Cumulative plots for bound and unbound times for different mutants. (a) Cumulative frequency plot for $t_{unbound}$ with different SD-aptamer distance (I1S8 to I6S8); (b) Cumulative frequency plot for t_{bound} with different SD-aptamer distance (I1S8 to I6S8). (c) Cumulative frequency plot for $t_{unbound}$ with different length of SD region (I4S8 to I4S0); (b) Cumulative frequency plot for t_{bound} with different SD-length (I4S8 to I4S0).

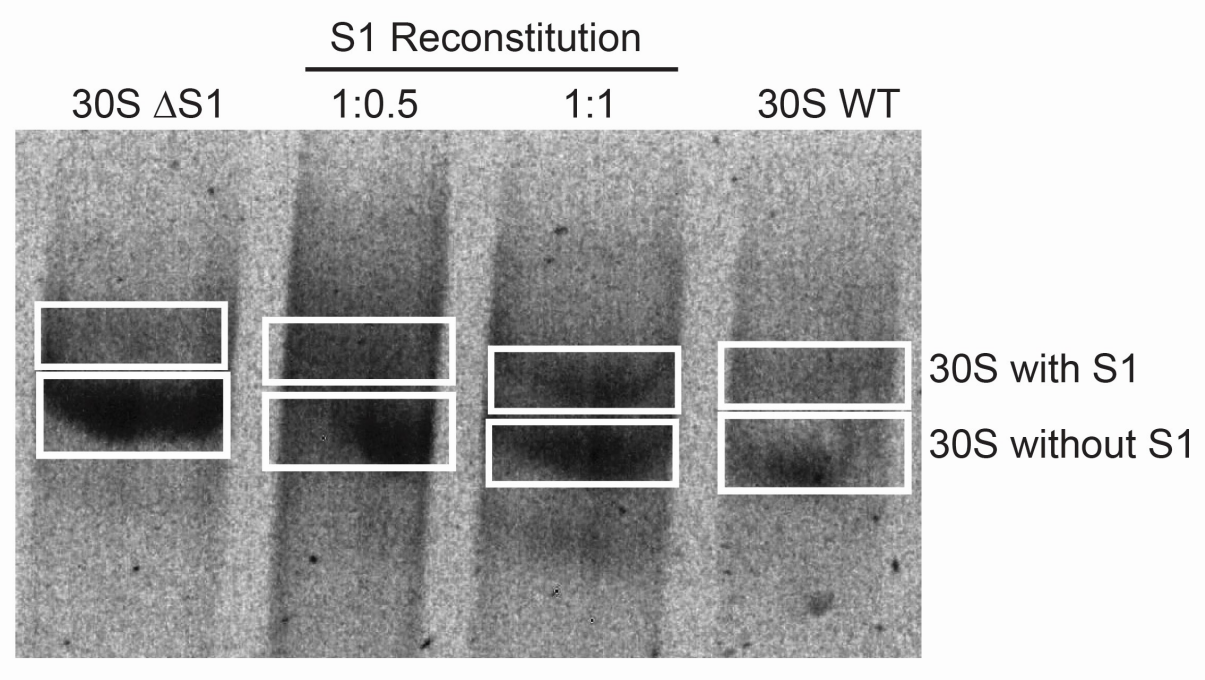

Supplementary Fig. 9| Assessment of S1 content in 30S subunits. S1 was first depleted from 30S to form 30S ΔS1 (first band). S1 was then restored by gradually adding purified 0.5-fold (second band) and 1X (third band) S1. Salt washed 30S WT (fourth band) shows the presence of 30S with and without S1.

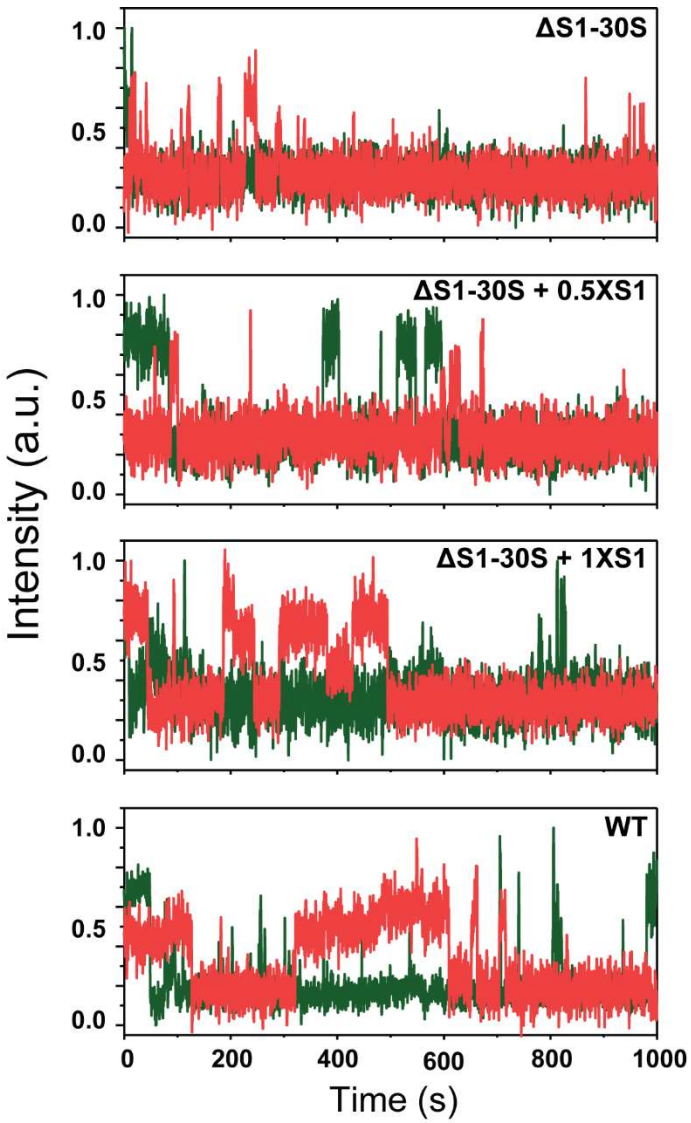

Supplementary Fig. 10| Reconstitution of S1 into 30S subunits. Incorporation of S1 at various molar ratio to ΔS1-30S increased the 30S binding to the R-mRNA^{+30}.

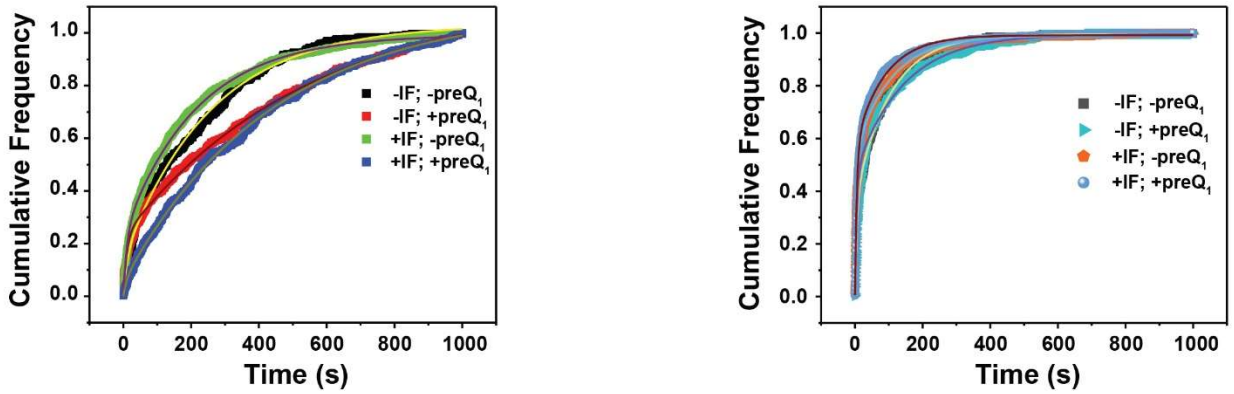

Supplementary Fig. 11| Cumulative plots for unbound times ($t_{unbound}$, left) and bound times (t_{bound}, right) without and with IFs and preQ$_1$.

$$R+S \underset{k_{-1}}{\overset{k_1}{\rightleftharpoons}} R{\cdot}S \underset{k_{-2}}{\overset{k_2}{\rightleftharpoons}} RS^*$$

$$K_1 = \frac{k_{-1}}{k_1} = \frac{[R][S]}{[R{\cdot}S]} = e^{\Delta G_{SC}/RT}$$

$$K_2 = \frac{k_{-2}}{k_2} = \frac{[R{\cdot}S]}{[RS^*]} = e^{\Delta G_{SI}/RT}$$

ΔG_{IA} = binding energy for initiation active complex.
ΔG_{SC} = binding energy for standby complex.
ΔG_{SI} = RNA unfolding energy.

$$\Delta G_{IA} = \Delta G_{SC} + \Delta G_{SI}$$

From our calculations rate values,
we found the energy values in unit of RT,

$\Delta G_{SC}^{-preQ1} = -3.6$ $\Delta G_{SC}^{+preQ1} = -3.6$
$\Delta G_{SI}^{-preQ1} = -0.5$ $\Delta G_{SI}^{+preQ1} = 0.9$
$\Delta G_{IA}^{-preQ1} = -4.1$ $\Delta G_{IA}^{+preQ1} = -2.7$

$$\Delta\Delta G_{unfolding\ penalty} = \Delta G_{SI}^{-preQ1} - \Delta G_{SI}^{+preQ1} = 1.4\ kcal/mole$$

Supplementary Fig. 12| Free Energy estimates of with and without $preQ_1$ conditions.

Supplementary Tables

Table S1. *List of RNA sequence used for microscopy and biochemistry. The captureing part of the mRNA is shown in gray, the aptamer is italized, the SD sequence is non-italizised and underlined, an insertion is bolded and highlighted in gray, the start codon is italized and green.*

Name	Sequence
WT R-mRNA^{+30} (I-2S8)	GGGCAGUGAGCAACAAAAUGC*UCACCUGGGUCGCAGUAACCCCAGUUAACA AAACA*AGGGAGGU*AAUUUUGUG*CCCAAAAAAAGAAUAAAAGAUUUAGCU
I1S8 R-mRNA	GGGCAGUGAGCAACAAAAUGC*UCACCUGGGUCGCAGUAACCCCAGUUAACA AAACAAG**U**AGGGAGGU*AAUUUUGUG*CCCAAAAAAAGAAUAAAAGAUUUAG CU
I2S8 R-mRNA	GGGCAGUGAGCAACAAAAUGC*UCACCUGGGUCGCAGUAACCCCAGUUAACA AAACAAG**AU**AGGGAGGU*AAUUUUGUG*CCCAAAAAAAGAAUAAAAGAUUUA GCU
I4S8 R-mRNA	GGGCAGUGAGCAACAAAAUGC*UCACCUGGGUCGCAGUAACCCCAGUUAACA AAACAAG**AUAU**AGGGAGGU*AAUUUUGUG*CCCAAAAAAAGAAUAAAAGAUU UAGCU
I6S8 R-mRNA	GGGCAGUGAGCAACAAAAUGC*UCACCUGGGUCGCAGUAACCCCAGUUAACA AAACAAG**AUAUAU**AGGGAGGU*AAUUUUGUG*CCCAAAAAAAGAAUAAAAGA UUUAGCU
I4S7 R-mRNA	GGGCAGUGAGCAACAAAAUGC*UCACCUGGGUCGCAGUAACCCCAGUUAACA AAACAAG**AUAU**UGGGAGGU*AAUUUUGUG*CCCAAAAAAAGAAUAAAAGAUU UAGCU
I4S6 R-mRNA	GGGCAGUGAGCAACAAAAUGC*UCACCUGGGUCGCAGUAACCCCAGUUAACA AAACAAG**AUAU**UUGGAGGU*AAUUUUGUG*CCCAAAAAAAGAAUAAAAGAUU UAGCU
I4S5 R-mRNA	GGGCAGUGAGCAACAAAAUGC*UCACCUGGGUCGCAGUAACCCCAGUUAACA AAACAAG**AUAU**UUUGAGGU*AAUUUUGUG*CCCAAAAAAAGAAUAAAAGAUU UAGCU
I4S0 R-mRNA	GGGCAGUGAGCAACAAAAUGC*UCACCUGGGUCGCAGUAACCCCAGUUAACA AAACAAG**AUAU**AUAUAUAUAAUUUUGUG*CCCAAAAAAAGAAUAAAAGAUU UAGCU
Capture Strand DNA	*5'-GCATTTTGTTGCTCACTGCCC-biotin-3'*
Capture Strand DNA with Cy3	*5'-Cy3-GCATTTTGTTGCTCACTGCCC-biotin-3'*
30S DNA labeling probe	*5' – Cy5- GGG AGA TCA GGA TA -Cy5 3'*

Table S2 A *List of all unbound times ($t_{unbound}$) and association rates (k_{on}) for 30S binding to R-mRNA^{+30} at different preQ$_1$ concentration.*

[PreQ$_1$] (nM)	$t_{unbound,slow}$ (s)	±Δ $t_{unbound,slow}$ (s)	A_1	±ΔA_1	$k_{on,slow}$ (×10^{6}M^{-1}s^{-1})	±Δ $k_{on,slow}$ (×10^{6}M^{-1}s^{-1})	$k_{on,slow}$ (PB corrected) (×10^{6}M^{-1}s^{-1})	±Δ $k_{on,slow}$ (PB corrected) (×10^{6}M^{-1}s^{-1})
0	299.9	35.3	0.89	0.04	0.17	0.02	0.33	0.04
50	410.8	19.3	0.93	0.03	0.12	0.01	0.28	0.01
100	424.2	38.8	0.83	0.05	0.12	0.01	0.27	0.03
200	490.5	92.8	0.85	0.05	0.10	0.02	0.26	0.05
500	539.9	36.8	0.85	0.05	0.09	0.01	0.25	0.02
1000	607.5	86.1	0.96	0.08	0.08	0.01	0.24	0.03

[PreQ$_1$] (nM)	$t^{shared}_{unbound,fast}$ (s)	±Δ $t^{shared}_{unbound,fast}$ (s)	A_2	±ΔA_2	$k_{on,fast}$ (×10^{6}M^{-1}s^{-1})	±Δ $k_{on,fast}$ (×10^{6}M^{-1}s^{-1})	$k_{on,fast}$ (PB corrected) (×10^{6}M^{-1}s^{-1})	±Δ $k_{on,fast}$ (PB corrected) (×10^{6}M^{-1}s^{-1})
0	10.3	1.38	0.15	0.03	4.85	0.65	4.84	0.65
50	10.3	1.38	0.15	0.02	4.85	0.65	4.84	0.65
100	10.3	1.38	0.29	0.04	4.85	0.65	4.84	0.65
200	10.3	1.38	0.24	0.03	4.85	0.65	4.84	0.65
500	10.3	1.38	0.10	0.01	4.85	0.65	4.84	0.65
1000	10.3	1.38	0.22	0.01	4.85	0.65	4.84	0.65

Table S2 B *List of all bound times (t_{bound}) and dissociation rates (k_{off}) for 30S binding to R-mRNA^{+30} at different preQ$_1$ concentration.*

[PreQ$_1$] (nM)	***$t_{bound,slow}$ (s)***	***±Δ $t_{bound,slow}$ (s)***	***A_1***	***±ΔA_1***	***$k_{off,slow}$ (s^{-1})***	***±Δ $k_{off,slow}$ (s^{-1})***	***$k_{off,slow}$ (PB Corrected) (s^{-1})***	***±Δ$k_{off,slow}$ (PB Corrected) (s^{-1})***
0	*137.2*	*41.3*	*0.58*	*0.08*	*0.007*	*0.002*	*0.002*	*0.001*
50	*110.8*	*29.9*	0.48	*0.07*	*0.009*	*0.002*	*0.004*	*0.001*
100	*96.2*	*58.9*	*0.41*	*0.03*	*0.012*	*0.002*	*0.005*	*0.003*
200	*100.1*	*16.3*	*0.48*	*0.06*	*0.010*	*0.002*	*0.005*	*0.001*
500	*90.7*	*18.5*	*0.49*	*0.01*	*0.007*	*0.001*	*0.006*	*0.001*
1000	*86.1*	*13.8*	*0.28*	*0.08*	*0.008*	*0.004*	*0.006*	*0.001*

[PreQ$_1$] (nM)	***$t^{shared}_{bound,fast}$ (s)***	***±Δ $t^{shared}_{bound,fast}$ (s)***	***A_2***	***±ΔA_2***	***$k_{off,fast}$ (s^{-1})***	***±Δ $k_{off,fast}$ (s^{-1})***	***$k_{off,fast}$ (PB Corrected) (s^{-1})***	***±Δ$k_{off,fast}$ (PB Corrected) (s^{-1})***
0	*7.2*	*1.10*	*0.36*	*0.03*	*0.138*	*0.021*	*0.133*	*0.020*
50	*7.2*	*1.10*	*0.51*	*0.07*	*0.138*	*0.021*	*0.133*	*0.020*
100	*7.2*	*1.10*	*0.58*	*0.08*	*0.138*	*0.021*	*0.133*	*0.020*
200	*7.2*	*1.10*	*0.51*	*0.07*	*0.138*	*0.021*	*0.133*	*0.020*
500	*7.2*	*1.10*	*0.38*	*0.10*	*0.138*	*0.021*	*0.133*	*0.020*
1000	*7.2*	*1.10*	*0.72*	*0.03*	*0.138*	*0.021*	*0.133*	*0.020*

Table S3 *Counts of short (represented in red) and long (represented in blue) binding events from the raster plot of 100 molecules in the absence and presence of $preQ_1$ added to R-mRNA^{+30}*

	Without $PreQ_1$			***With $PreQ_1$***		
Total Molecules	*# of short binding*	*# of long binding*	*Total binding*	*# of short binding*	*# of long binding*	*Total binding*
100	*194*	*97*	*291*	*184*	*65*	*248*

Table S4 A Ligand Jump Experiments. *Transition of accessibility with and without $preQ_1$*

Without $PreQ_1$ (Before ligand flow)			***With $PreQ_1$ (After ligand flow)***		
			Low	*Mid*	*High*
Low	*102 (45%)*	Transition →	*90*	*11*	*1*
Mid	*70 (31%)*		*62*	*6*	*2*
High	*55 (24%)*		*35*	*11*	*9*
			187 (82%)	*28 (12%)*	*12 (6%)*
46% molecules stay in the same rank (Low → Low, Mid → Mid, High → High). *48% molecules have reduced accessibility rank (Mid → Low, High → Low/Mid).* *6% molecules have increased accessibility rank (Low → Mid/ High, Mid → High).*					
15% molecule transition to completely inaccessible 30S binding once $preQ_1$ is introduced.					

Table S4 B Ligand Jump Experiments. *Counts of short (represented in red) and long (represented in blue) binding events from the raster plot of 100 molecules in the absence and presence of $preQ_1$ to R-mRNA^{+30}*

	Without $PreQ_1$ (Before ligand flow)				***With $PreQ_1$ (After ligand flow)***			
	# of total molecules	*# of short binding*	*# of long binding*	*Total binding*	*# of total molecules*	*# of short binding*	*# of long binding*	*Total binding*
Total	*100*	*506*	*254*	*760*	*100*	*356*	*107*	*463*

Table S5. *Table of site-directed mutagenesis primers used to generate mutant aptamer series of plasmids*

Primer Sample	**Primer Sequence (5' to 3')**
Tte_Forward primer	/5Phos/ GAGGTAATTTTGTGCCC
Tte_I1S8 Reverse Primer	/5Phos/ CCTACTTGTTTTGTTAACTGG
Tte_I2S8 Reverse Primer	/5Phos/ CCTATCTTGTTTTGTTAACTGG
Tte_I4S8 Reverse Primer	/5Phos/ CCTATATCTTGTTTTGTTAACTGG

Tte_I6S8 Reverse Primer	/5Phos/ CCTATATATCTTGTTTTGTTAACTGG
Tte_I4S7 Reverse Primer	/5Phos/ CCAATATCTTGTTTTGTTAACTGG
Tte_I4S6 Reverse Primer	/5Phos/ CAAATATCTTGTTTTGTTAACTGG
Tte_I4S5 Forward Primer	/5Phos/ CCAAAAAAAGAATAAAAGATTTAGC
Tte_I4S5 Reverse Primer	/5Phos/ GCACAAAATTACCTCAAAATATCTTG
Tte_I4S0 Reverse Primer	/5Phos/ GCACAAAATTATATATATATATATCTTGTTTTGTTAAC

Table S6 A *List of all unbound times ($t_{unbound}$) and association rates (k_{on}) for mutants with different SD-aptamer distance (I1S8 to I6S8)*

	$t_{unbound,\ slow}$ (s)	±Δ $t_{unbound,slow}$ (s)	A_1	±ΔA_1	$k_{on,slow}$ ($\times10^6 M^{-1}s^{-1}$)	±Δ $k_{on,slow}$ ($\times10^6 M^{-1}s^{-1}$)	$k_{on,slow}$ (PB corrected) ($\times10^6 M^{-1}s^{-1}$)	±Δ $k_{on,slow}$ (PB corrected) ($\times10^6 M^{-1}s^{-1}$)
I1S8	558.7	55.6	0.79	0.02	0.089	0.009	0.248	0.025
I2S8	327.4	11.2	0.79	0.02	0.153	0.005	0.311	0.011
I4S8	247.3	9.4	0.62	0.01	0.202	0.008	0.361	0.014
I6S8	277.7	10.6	0.64	0.01	0.180	0.007	0.338	0.013

	$t^{shared}_{unbound,fast}$ (s)	±Δ $t^{shared}_{unbound,fast}$ (s)	A_2	±ΔA_2	$k_{on,fast}$ ($\times10^6 M^{-1}s^{-1}$)	±Δ $k_{on,fast}$ ($\times10^6 M^{-1}s^{-1}$)	$k_{on,fast}$ (PB corrected) ($\times10^6 M^{-1}s^{-1}$)	±Δ $k_{on,fast}$ (PB corrected) ($\times10^6 M^{-1}s^{-1}$)
I1S8	16.5	1.53	0.25	0.01	3.034	0.283	3.189	0.296
I2S8	16.5	1.53	0.21	0.01	3.034	0.283	3.189	0.296
I4S8	16.5	1.53	0.37	0.01	3.034	0.283	3.189	0.296
I6S8	16.5	1.53	0.35	0.01	3.034	0.283	3.189	0.296

Table S6 B *List of all bound times (t_{bound}) and dissociation rates (k_{off}) for mutants with different SD-aptamer distance (I1S8 to I6S8)*

	$t_{bound,\ slow}$ (s)	±Δ $t_{bound,slow}$ (s)	A_1	±ΔA_1	$k_{off,slow}$ ($\times10^6 M^{-1}s^{-1}$)	±Δ $k_{off,slow}$ ($\times10^6 M^{-1}s^{-1}$)	$k_{off,slow}$ (PB corrected)	±Δ $k_{off,slow}$ (PB corrected)

							($\times 10^6 M^{-1}s^{-1}$)	($\times 10^6 M^{-1}s^{-1}$)
I1S8	84.8	20.2	0.48	0.02	0.012	0.003	0.007	0.002
I2S8	58.2	8.0	0.33	0.03	0.017	0.002	0.012	0.002
I4S8	99.3	37.5	0.30	0.01	0.010	0.004	0.005	0.002
I6S8	74.5	42.8	0.19	0.07	0.013	0.008	0.008	0.005

	$t_{bound,fast}^{shared}$ (s)	$\pm\Delta$ $t_{bound,fast}^{shared}$ (s)	A_2	$\pm\Delta A_2$	$k_{off,fast}$ ($\times 10^6 M^{-1}s^{-1}$)	$\pm\Delta$ $k_{off,fast}$ ($\times 10^6 M^{-1}s^{-1}$)	$k_{off,fast}$ (PB corrected) ($\times 10^6 M^{-1}s^{-1}$)	$\pm\Delta$ $k_{off,fast}$ (PB corrected) ($\times 10^6 M^{-1}s^{-1}$)
I1S8	2.3	0.85	0.52	0.02	0.435	0.162	0.429	0.159
I2S8	2.3	0.85	0.66	0.03	0.435	0.162	0.429	0.159
I4S8	2.3	0.85	0.70	0.01	0.435	0.162	0.429	0.159
I6S8	2.3	0.85	0.81	0.07	0.435	0.162	0.429	0.159

Table S7 *Counts of short (represented in red) and long (represented in blue) binding events from the raster plot of 100 molecules for the two set of mutants with minimum SD-aptamer separation (I1S8) to maximum SD-aptamer separation (I6S8)*

	I1S8			**I6S8**		
Total Molecules	*# of short binding*	*# of long binding*	*Total binding*	*# of short binding*	*# of long binding*	*Total binding*
100	190	112	302	651	119	770

Table S8 A *List of all unbound times ($t_{unbound}$) and association rates (k_{on}) for mutants with different SD-aptamer distance (I4S8 to I4S0)*

	$t_{unbound,slow}$ (s)	$\pm\Delta$ $t_{unbound,slow}$ (s)	A_1	$\pm\Delta A_1$	$k_{on,slow}$ ($\times 10^6 M^{-1}s^{-1}$)	$\pm\Delta$ $k_{on,slow}$ ($\times 10^6 M^{-1}s^{-1}$)	$k_{on,slow}$ (PB corrected) ($\times 10^6 M^{-1}s^{-1}$)	$\pm\Delta$ $k_{on,slow}$ (PB corrected) ($\times 10^6 M^{-1}s^{-1}$)
I4S8	248.1	6.7	0.63	0.02	0.202	0.006	0.359	0.009
I4S7	284.3	6.3	0.60	0.02	0.176	0.004	0.334	0.007
I4S6	342.1	17.2	0.67	0.03	0.146	0.007	0.304	0.015
I4S5	369.4	30.4	0.63	0.01	0.135	0.011	0.297	0.024
I4S0	484.1	35.5	0.81	0.02	0.103	0.008	0.262	0.019

	$t_{unbound,fast}^{shared}$ (s)	$\pm\Delta$ $t_{unbound,fast}^{shared}$ (s)	A_2	$\pm\Delta A_2$	$k_{on,fast}$ ($\times 10^6 M^{-1}s^{-1}$)	$\pm\Delta$ $k_{on,fast}$ ($\times 10^6 M^{-1}s^{-1}$)	$k_{on,fast}$ (PB corrected) ($\times 10^6 M^{-1}s^{-1}$)	$\pm\Delta$ $k_{on,fast}$ (PB corrected) ($\times 10^6 M^{-1}s^{-1}$)
I4S8	16.24	1.23	0.37	0.02	3.078	0.233	3.237	0.245

I4S7	*16.24*	*1.23*	*0.40*	*0.02*	*3.078*	*0.233*	*3.237*	*0.245*
I4S6	*16.24*	*1.23*	*0.34*	*0.02*	*3.078*	*0.233*	*3.237*	*0.245*
I4S5	*16.24*	*1.23*	*0.37*	*0.01*	*3.078*	*0.233*	*3.237*	*0.245*
I4S0	*16.24*	*1.23*	*0.22*	*0.01*	*3.078*	*0.233*	*3.237*	*0.245*

Table S8 B *List of all bound times (t_{bound}) and dissociation rates (k_{off}) for mutants with different SD-aptamer distance (I4S8 to I4S0)*

	$t_{bound,slow}$ (s)	±Δ $t_{bound,slow}$ (s)	A_1	±ΔA_1	$k_{off,slow}$ ($\times10^6 M^{-1}s^{-1}$)	±Δ $k_{off,slow}$ ($\times10^6 M^{-1}s^{-1}$)	$k_{off,slow}$ (PB corrected) ($\times10^6 M^{-1}s^{-1}$)	±Δ $k_{off,slow}$ (PB corrected) ($\times10^6 M^{-1}s^{-1}$)
I4S8	*114.9*	*43. 1*	*0.32*	*0.02*	*0.009*	*0.003*	*0.004*	*0.001*
I4S7	*53.6*	*4.1*	*0.30*	*0.02*	*0.019*	*0.001*	*0.014*	*0.001*
I4S6	*57.8*	*11.2*	*0.17*	*0.02*	*0.017*	*0.003*	*0.012*	*0.002*
I4S5	*131.7*	*42.6*	*0.45*	*0.03*	*0.008*	*0.002*	*0.003*	*0.001*
I4S0	*64.5*	*6.9*	*0.24*	*0.02*	*0.016*	*0.002*	*0.011*	*0.001*

	$t^{shared}_{bound,fast}$ (s)	±Δ $t^{shared}_{bound,fast}$ (s)	A_2	±ΔA_2	$k_{off,fast}$ ($\times10^6 M^{-1}s^{-1}$)	±Δ $k_{off,fast}$ ($\times10^6 M^{-1}s^{-1}$)	$k_{off,fast}$ (PB corrected) ($\times10^6 M^{-1}s^{-1}$)	±Δ $k_{off,fast}$ (PB corrected) ($\times10^6 M^{-1}s^{-1}$)
I4S8	*1.72*	*0.20*	*0.67*	*0.02*	*0.582*	*0.067*	*0.577*	*0.067*
I4S7	*1.72*	*0.20*	*0.70*	*0.02*	*0.582*	*0.067*	*0.577*	*0.067*
I4S6	*1.72*	*0.20*	*0.82*	*0.02*	*0.582*	*0.067*	*0.577*	*0.067*
I4S5	*1.72*	*0.20*	*0.54*	*0.03*	*0.582*	*0.067*	*0.577*	*0.067*
I4S0	*1.72*	*0.20*	*0.73*	*0.02*	*0.582*	*0.067*	*0.577*	*0.067*

Table S9 *Counts of short (represented in red) and long (represented in blue) binding events from the raster plot of 100 molecules for the two set of mutants with fully available SD-aptamer complementarity (I4S8) to no SD-aptamer complementarity (I4S0)*

	I4S8			***I4S0***		
Total Molecules	*# of short binding*	*# of long binding*	*Total binding*	*# of short binding*	*# of long binding*	*Total binding*
100	*527*	*81*	*608*	*253*	*45*	*248*

Table S10 A *Unbound times (t_{bound}) and association rates (k_{on}) for the influence of $preQ_1$ on mutant I1S8*

	$t_{unbound,slow}$ (s)	±Δ $t_{unbound,slow}$ (s)	A_1	±ΔA_1	$k_{on,slow}$ ($\times10^6 M^{-1}s^{-1}$)	±Δ $k_{on,slow}$ ($\times10^6 M^{-1}s^{-1}$)	$k_{on,slow}$ (PB corrected) ($\times10^6 M^{-1}s^{-1}$)	±Δ $k_{on,slow}$ (PB corrected) ($\times10^6 M^{-1}s^{-1}$)
I1S8 -$preQ_1$	*330.9*	*61.0*	*0.51*	*0.03*	*0.151*	*0.028*	*0.309*	*0.057*
I1S8 +$preQ_1$	*290.9*	*46.1*	*0.52*	*0.01*	*0.172*	*0.027*	*0.330*	*0.052*

	$t^{shared}_{unbound,fas}$ (s)	±Δ $t^{shared}_{unbound,fast}$ (s)	A_2	±ΔA_2	$k_{on,fast}$ (×$10^6 M^{-1}s^{-1}$)	±Δ $k_{on,fast}$ (×$10^6 M^{-1}s^{-1}$)	$k_{on,fast}$ (PB corrected) (×$10^6 M^{-1}s^{-1}$)	±Δ $k_{on,fast}$ (PB corrected) (×$10^6 M^{-1}s^{-1}$)
I1S8 -preQ$_1$	*7.8*	*1.63*	*0.49*	*0.03*	*6.389*	*1.331*	*6.569*	*1.373*
I1S8 +preQ$_1$	*7.8*	*1.63*	*0.48*	*0.01*	*6.389*	*1.331*	*6.569*	*1.373*

Table S10 B *Bound times (t_{bound}) and dissociation rates (k_{off}) for the influence of preQ$_1$ on mutant I1S8*

	$t_{bound,\ slow}$ (s)	±Δ $t_{bound,slow}$ (s)	A_1	±ΔA_1	$k_{off,slow}$ (×$10^6 M^{-1}s^{-1}$)	±Δ $k_{off,slow}$ (×$10^6 M^{-1}s^{-1}$)	$k_{off,slow}$ (PB corrected) (×$10^6 M^{-1}s^{-1}$)	±Δ $k_{off,slow}$ (PB corrected) (×$10^6 M^{-1}s^{-1}$)
I1S8 -preQ$_1$	*168.3*	*7.5*	*0.59*	*0.02*	*0.006*	*0.001*	*0.001*	*0.001*
I1S8 +preQ$_1$	*219.0*	*23.0*	*0.46*	*0.01*	*0.005*	*0.001*	*0.001*	*0.001*

	$t^{shared}_{bound,fast}$ (s)	±Δ $t^{shared}_{bound,fast}$ (s)	A_2	±ΔA_2	$k_{off,fast}$ (×$10^6 M^{-1}s^{-1}$)	±Δ $k_{off,fast}$ (×$10^6 M^{-1}s^{-1}$)	$k_{off,fast}$ (PB corrected) (×$10^6 M^{-1}s^{-1}$)	±Δ $k_{off,fast}$ (PB corrected) (×$10^6 M^{-1}s^{-1}$)
I1S8 -preQ$_1$	*5.8*	*0.51*	*0.39*	*0.02*	*0.172*	*0.015*	*0.167*	*0.015*
I1S8 +preQ$_1$	*5.8*	*0.51*	*0.53*	*0.01*	*0.172*	*0.015*	*0.167*	*0.015*

Table S11 A *Unbound times ($t_{unbound}$) and association rates (k_{on}) for the influence of preQ$_1$ on mutant construct I4S8*

	$t_{unbound,\ slow}$ (s)	±Δ $t_{unbound,slow}$ (s)	A_1	±ΔA_1	$k_{on,slow}$ (×$10^6 M^{-1}s^{-1}$)	±Δ $k_{on,slow}$ (×$10^6 M^{-1}s^{-1}$)	$k_{on,slow}$ (PB corrected) (×$10^6 M^{-1}s^{-1}$)	±Δ $k_{on,slow}$ (PB corrected) (×$10^6 M^{-1}s^{-1}$)
I4S8 -preQ$_1$	*385.0*	*31.4*	*0.54*	*0.01*	*0.129*	*0.011*	*0.288*	*0.024*

I4S8 +preQ$_1$	*403.0*	*20.7*	*0.53*	*0.02*	*0.124*	*0.006*	*0.282*	*0.015*

	$t_{unbound,fa}^{shared}$ (s)	±Δ $t_{unbound,fast}^{shared}$ (s)	A_2	±ΔA_2	$k_{on,fast}$ (×10^{6}M^{-1}s^{-1})	±Δ $k_{on,fast}$ (×10^{6}M^{-1}s^{-1})	$k_{on,fast}$ (PB corrected) (×10^{6}M^{-1}s^{-1})	±Δ $k_{on,fast}$ (PB corrected) (×10^{6}M^{-1}s^{-1})
I4S8 -preQ$_1$	*9.6*	*1.6*	*0.45*	*0.018*	*5.192*	*0.869*	*5.367*	*0.894*
I4S8 +preQ$_1$	*9.6*	*1.6*	*0.48*	*0.020*	*5.192*	*0.869*	*5.367*	*0.894*

Table S11 B *Bound times (t_{bound}) and dissociation rates (k_{off}) for the influence of preQ$_1$ on mutant construct I4S8*

	$t_{bound,slow}$ (s)	±Δ $t_{bound,slow}$ (s)	A_1	±ΔA_1	$k_{off,slow}$ (×10^{6}M^{-1}s^{-1})	±Δ $k_{off,slow}$ (×10^{6}M^{-1}s^{-1})	$k_{off,slow}$ (PB corrected) (×10^{6}M^{-1}s^{-1})	±Δ $k_{off,slow}$ (PB corrected) (×10^{6}M^{-1}s^{-1})
I4S8 -preQ$_1$	*162.9*	*21.5*	*0.51*	*0.03*	*0.006*	*0.001*	*0.001*	*0.0001*
I4S8 +preQ$_1$	*138.9*	*19.1*	*0.52*	*0.02*	*0.007*	*0.001*	*0.002*	*0.0003*

	$t_{bound,fa}^{shared}$ (s)	±Δ $t_{bound,fast}^{shared}$ (s)	A_2	±ΔA_2	$k_{off,fast}$ (×10^{6}M^{-1}s^{-1})	±Δ $k_{off,fast}$ (×10^{6}M^{-1}s^{-1})	$k_{off,fast}$ (PB corrected) (×10^{6}M^{-1}s^{-1})	±Δ $k_{off,fast}$ (PB corrected) (×10^{6}M^{-1}s^{-1})
I4S8 -preQ$_1$	*4.1*	*0.74*	*0.49*	*0.03*	*0.245*	*0.045*	*0.239*	*0.043*
I4S8 +preQ$_1$	*4.1*	*0.74*	*0.47*	*0.02*	*0.245*	*0.045*	*0.239*	*0.043*

Table S12 A *Unbound times ($t_{unbound}$) and associated rates (k_{on}) of 30S interaction with R-mRNA^{+30} under the influence of S1 protein*

	$t_{unbound,slow}$ (s)	±Δ $t_{unbound,slow}$ (s)	A_1	±ΔA_1	$k_{on,slow}$ (×10^{6}M^{-1}s^{-1})	±Δ $k_{on,slow}$ (×10^{6}M^{-1}s^{-1})	$k_{on,slow}$ (PB corrected) (×10^{6}M^{-1}s^{-1})	±Δ $k_{on,slow}$ (PB corrected) (×10^{6}M^{-1}s^{-1})
ΔS1-30S	*622.3*	*1.85*	*1.27*	*0.00*	*0.080*	*0.001*	*0.239*	*0.001*
ΔS1-30S+0.5x purified S1	*605.9*	*2.09*	*1.06*	*0.00*	*0.083*	*0.001*	*0.241*	*0.001*

ΔS1-30S+1x purified S1	*531.3*	*1.80*	*0.93*	*0.00*	*0.094*	*0.001*	*0.252*	*0.001*
WT-30S	*299.9*	*35.26*	*0.90*	*0.04*	*0.167*	*0.019*	*0.325*	*0.038*

	$t^{shared}_{unbound,fa}$ (s)	±Δ $t^{shared}_{unbound,fast}$ (s)	A_2	±ΔA_2	$k_{on,fast}$ (×$10^6 M^{-1}s^{-1}$)	±Δ $k_{on,fast}$ (×$10^6 M^{-1}s^{-1}$)	$k_{on,fast}$ (PB corrected) (×$10^6 M^{-1}s^{-1}$)	±Δ $k_{on,fast}$ (PB corrected) (×$10^6 M^{-1}s^{-1}$)
ΔS1-30S	*10.31*	*1.10*	*0.03*	*0.03*	*4.85*	*0.52*	*5.01*	*0.54*
ΔS1-30S+0.5x purified S1	*10.31*	*1.10*	*0.17*	*0.03*	*4.85*	*0.52*	*5.01*	*0.54*
ΔS1-30S+1x purified S1	*10.31*	*1.10*	*0.23*	*0.03*	*4.85*	*0.52*	*5.01*	*0.54*
WT-30S	*10.31*	*1.38*	*0.15*	*0.03*	*4.85*	*0.65*	*5.01*	*0.67*

Table S12 B *Bound times (t_{bound}) and dissociated rates (k_{off}) of 30S interaction with R-mRNA^{+30} under the influence of S1 protein*

	$t_{bound,slow}$ (s)	±Δ $t_{bound,slow}$ (s)	A_1	±ΔA_1	$k_{off,slow}$ (×$10^6 M^{-1}s^{-1}$)	±Δ $k_{off,slow}$ (×$10^6 M^{-1}s^{-1}$)	$k_{off,slow}$ (PB corrected) (×$10^6 M^{-1}s^{-1}$)	±Δ $k_{off,slow}$ (PB corrected) (×$10^6 M^{-1}s^{-1}$)
ΔS1-30S	*66.8*	*0.6*	*0.25*	*0.001*	*0.015*	*0.001*	*0.010*	*0.001*
ΔS1-30S+0.5x purified S1	*68.3*	*0.3*	*0.53*	*0.001*	*0.015*	*0.001*	*0.009*	*0.001*
ΔS1-30S+1x purified S1	*103.2*	*0.3*	*0.64*	*0.001*	*0.009*	*0.001*	*0.005*	*0.001*
WT-30S	*137.2*	*41.3*	*0.58*	*0.084*	*0.007*	*0.002*	*0.002*	*0.003*

	$t^{shared}_{bound,fast}$ (s)	±Δ $t^{shared}_{bound,fast}$ (s)	A_2	±ΔA_2	$k_{off,fast}$ (×$10^6 M^{-1}s^{-1}$)	±Δ $k_{off,fast}$ (×$10^6 M^{-1}s^{-1}$)	$k_{off,fast}$ (PB corrected) (×$10^6 M^{-1}s^{-1}$)	±Δ $k_{off,fast}$ (PB corrected) (×$10^6 M^{-1}s^{-1}$)
ΔS1-30S	7.22	1.10	0.74	0.001	0.138	0.021	0.133	0.020
ΔS1-30S+0.5x purified S1	7.22	1.10	0.40	0.003	0.138	0.021	0.133	0.020
ΔS1-30S+1x purified S1	7.22	1.10	0.27	0.003	0.138	0.021	0.133	0.020
WT-30S	7.22	1.10	0.36	0.034	0.138	0.021	0.133	0.020

Table S13 A *Unbound times ($t_{unbound}$) and associated rates (k_{on}) for the influence of $preQ_1$ in absence and presence of initiation factors (IFs)*

	$t_{unbound,\ slow}$ (s)	±Δ $t_{unbound,slow}$ (s)	A_1	±ΔA_1	$k_{on,slow}$ ($\times10^6 M^{-1}s^{-1}$)	±Δ $k_{on,slow}$ ($\times10^6 M^{-1}s^{-1}$)	$k_{on,slow}$ (PB corrected) ($\times10^6 M^{-1}s^{-1}$)	±Δ $k_{on,slow}$ (PB corrected) ($\times10^6 M^{-1}s^{-1}$)
-IF; -$preQ_1$	299.9	35.3	0.89	0.04	0.167	0.019	0.325	0.038
-IF; +$preQ_1$	607.5	86.1	0.96	0.08	0.082	0.012	0.241	0.034
+IF; -$preQ_1$	220.3	7.2	0.76	0.03	0.227	0.007	0.385	0.013
+IF; +$preQ_1$	460.8	72.6	1.04	0.06	0.108	0.017	0.267	0.042

	$t^{shared}_{unbound,fast}$ (s)	±Δ $t^{shared}_{unbound,fast}$ (s)	A_2	±ΔA_2	$k_{on,fast}$ ($\times10^6 M^{-1}s^{-1}$)	±Δ $k_{on,fast}$ ($\times10^6 M^{-1}s^{-1}$)	$k_{on,fast}$ (PB corrected) ($\times10^6 M^{-1}s^{-1}$)	±Δ $k_{on,fast}$ (PB corrected) ($\times10^6 M^{-1}s^{-1}$)
-IF; -$preQ_1$	10.3	1.38	0.15	0.03	4.851	0.645	4.845	0.649
-IF; +$preQ_1$	10.3	1.38	0.22	0.01	4.851	0.645	4.845	0.649
+IF; -$preQ_1$	10.3	1.38	0.30	0.02	4.851	0.645	4.845	0.649
+IF; +$preQ_1$	10.3	1.38	0.07	0.01	4.851	0.645	4.845	0.649

Table S13 B *Bound times (t_{bound}) and dissociated rates (k_{off}) for the influence of $preQ_1$ in absence and presence of initiation factors (IFs)*

	$t_{bound,\ slow}$ (s)	±Δ $t_{bound,slow}$ (s)	A_1	±ΔA_1	$k_{off,slow}$ ($\times10^6 M^{-1}s^{-1}$)	±Δ $k_{off,slow}$ ($\times10^6 M^{-1}s^{-1}$)	$k_{off,slow}$ (PB corrected) ($\times10^6 M^{-1}s^{-1}$)	±Δ $k_{off,slow}$ (PB corrected) ($\times10^6 M^{-1}s^{-1}$)
-IF; -$preQ_1$	137.2	41.3	0.58	0.08	0.007	0.002	0.002	0.001
-IF; +$preQ_1$	126.2	58.9	0.41	0.08	0.008	0.004	0.006	0.001
+IF; -$preQ_1$	98.8	13.9	0.42	0.04	0.010	0.001	0.005	0.001
+IF; +$preQ_1$	129.4	39.9	0.50	0.06	0.008	0.002	0.003	0.001

	$t^{shared}_{bound,fast}$ (s)	±Δ $t^{shared}_{bound,fast}$ (s)	A_2	±ΔA_2	$k_{off,fast}$ ($\times10^6 M^{-1}s^{-1}$)	±Δ $k_{off,fast}$ ($\times10^6 M^{-1}s^{-1}$)	$k_{off,fast}$ (PB corrected)	±Δ $k_{off,fast}$ (PB corrected)

							(×10^{6}M^{-1}s^{-1})	***(×10^{6}M^{-1}s^{-1})***
-IF; -preQ$_1$	*7.2*	*1.10*	*0.36*	*0.03*	*0.138*	*0.021*	*0.133*	*0.020*
-IF; +preQ$_1$	*7.2*	*1.10*	*0.58*	*0.08*	*0.138*	*0.021*	*0.133*	*0.020*
+IF; -preQ$_1$	*7.2*	*1.10*	*0.57*	*0.04*	*0.138*	*0.021*	*0.133*	*0.020*
+IF; +preQ$_1$	*7.2*	*1.10*	*0.46*	*0.06*	*0.138*	*0.021*	*0.133*	*0.020*

References

1. Dorywalska, M. et al. Site-specific labeling of the ribosome for single-molecule spectroscopy. *Nucleic Acids Res* **33**, 182-9 (2005).
2. Blanchard, S.C., Kim, H.D., Gonzalez, R.L., Jr., Puglisi, J.D. & Chu, S. tRNA dynamics on the ribosome during translation. *Proc Natl Acad Sci U S A* **101**, 12893-8 (2004).
3. Willkomm, D.K. & Hartmann, R.K. 3'-Terminal Attachment of Fluorescent Dyes and Biotin. in *Handbook of RNA Biochemistry* 117-128 (2014).
4. Bevilacqua, P.C. & Cech, T.R. Minor-groove recognition of double-stranded RNA by the double-stranded RNA-binding domain from the RNA-activated protein kinase PKR. *Biochemistry* **35**, 9983-94 (1996).
5. Wong, I. & Lohman, T.M. A double-filter method for nitrocellulose-filter binding: application to protein-nucleic acid interactions. *Proceedings of the National Academy of Sciences* **90**, 5428-5432 (1993).
6. Rio, D.C. Filter-binding assay for analysis of RNA-protein interactions. *Cold Spring Harb Protoc* **2012**, 1078-81 (2012).
7. Chandradoss, S.D. et al. Surface passivation for single-molecule protein studies. *J Vis Exp* (2014).
8. Roy, R., Hohng, S. & Ha, T. A practical guide to single-molecule FRET. *Nat Methods* **5**, 507-16 (2008).
9. Verveer, P.J. & Bastiaens, P.I.H. Evaluation of global analysis algorithms for single frequency fluorescence lifetime imaging microscopy data. *Journal of Microscopy* **209**, 1-7 (2003).
10. Verveer, P.J., Squire, A. & Bastiaens, P.I.H. Global Analysis of Fluorescence Lifetime Imaging Microscopy Data. *Biophysical Journal* **78**, 2127-2137 (2000).
11. Duss, O. et al. Real-time assembly of ribonucleoprotein complexes on nascent RNA transcripts. *Nature Communications* **9**, 5087 (2018).
12. Rinaldi, A.J., Lund, P.E., Blanco, M.R. & Walter, N.G. The Shine-Dalgarno sequence of riboswitch-regulated single mRNAs shows ligand-dependent accessibility bursts. *Nat Commun* **7**, 8976 (2016).